

Effect of Fascicle Length Range on Force Generation of Model-Based Biomimetic Controller for Tendon-Driven Prosthetic Hand*

Qi Luo, Chuanxin M. Niu, *Member, IEEE*, and Ning Lan, *Senior Member, IEEE*

Abstract—Model-based biomimetic control with neuromuscular reflex requires accurate representation of muscle fascicle length, which affects both force generation capability of muscle and dynamics of muscle spindle. However, physiological data are insufficient to guide the selection of range of fascicle length for task control. Here a reverse engineering approach was used to investigate the effects of different fascicle length range on controller's force control ability, so as to justify the selection of operating range of muscle length for a grasp force task. We compared 3 different ranges of fascicle length for their effects on force generation, i.e. R_1 : $0.5 - 1.0 L_0$, R_2 : $0.5 - 1.3 L_0$ and R_3 : $0.5 - 1.6 L_0$. The rationale to test these range selections was based on both physiological realism and engineering considerations. The steady state force output and transient force responses were evaluated with a range of step inputs as controller input. Results show that the prosthetic finger can produce a linear steady state force response with all 3 ranges of fascicle length. Peak force was the largest with R_3 . Fascicle length range had no significant effect on the rise time in force generation tasks. Results suggest that a wider range of fascicle length may be more favorable for force capacity, since the contact point of force control may well fall near the optimal length (L_0) region.

Clinical Relevance—This approach may eventually restore disrupted neuromechanics in amputees for control of prosthetic hands.

I. INTRODUCTION

Emulating human neuromuscular reflex following computational models may provide human-like compliance in prosthetic hands [1], [2]. In the model-based controller, the muscle fascicle length played an important role for reflex: it was the source of proprioception that should be explicitly provided to the muscle spindle [3]–[6], and the fascicle length must be accessible by the muscle model to engage force-length property [5], [7], [8]. The exact range of fascicle length, however, was unclear from literature. Therefore, ambiguity in fascicle length may yield muscle forces that are potentially unexplainable. In dynamic tasks such as finger pressing, it can be even more difficult to empirically determine the fascicle length of muscle, mainly due to scanty evidence of fascicle length from movement studies.

In search for a viable range of fascicle length during model-based prosthetic control, it might be useful (and inevitable) to allocate different ranges of fascicle length *a priori*. Pre-allocated ranges with better closed-loop behaviors can be reverse engineered to dissect their relevance to literature. The terminology of fascicle length in literature has

been somewhat inconsistent. For the length of muscle contractile element, hereby termed “fascial length”, the variations of terminology include “muscle length” [8], “muscle fiber length” [8], “fascicle length” [4], “contractile element” [5], [9], etc.

Following this *a priori* approach, previous study allocated a range of $0.5 - 1.6L_0$ to the fascicle length, which corresponded to $0^\circ - 60^\circ$ rotation of metacarpophalangeal (MCP) joint, $0 - 1.6$ cm translational displacement in the cable [1]. This range centered around L_0 , which was close to the maximal range supported by previous experiments [8]. However, this range contributed a negative component to the overall muscle stiffness [8], which may reduce the capacity of force generation. Therefore, there might exist other ranges of fascicle length that may generate larger force during finger pressing.

In this paper, we described the methodology of how to pre-allocate fascicle length in the model-based controller, especially how to reconcile the length conversion from real-world to model. Three ranges of fascicle length (R_1 : $0.5 - 1.0 L_0$; R_2 : $0.5 - 1.3 L_0$; R_3 : $0.5 - 1.6 L_0$) were introduced. We examined their effects on force generation with a tendon-driven prosthetic hand. R_1 engages only positive stiffness resulted from active muscle force; R_2 and R_3 both included negative stiffness regions, but the coverage was different. Force generation was tested by driving the prosthetic finger to press against a force transducer. We focus on whether different ranges of fascicle length would affect the static and dynamic performance of force generating during finger pressing. Results are expected to provide a reference for selection of fascicle length that could optimize the force generation capability of prosthetic hand.

II. METHODS

A. Tendon-driven Prosthetic Hand

Tendon-driven prosthetic hands are favored for model-based biomimetic control. This is because tendon-driven mechanisms are compatible with tendon-driven fingers in back-drivability; also the translational movement on a cable is compatible with the lengthening of a muscle. We adopted an open-source 3D-printed tendon-driven hand (InMoov).

In our implementation, hand joints were pulled using cables as proxies of human tendon, each of which simultaneously flexed the MCP, distal interphalangeal (DIP),

* This work was supported in part by a grant of the National Key R&D Program of China by the Ministry of Science and Technology of China (No.2017YFA0701103), a key grant from the Natural Science Foundation of China (No. 81630050), and a grant from the Institute of Medical Robotics of Shanghai Jiao Tong University (No. IMR2018KY01).

Q. Luo, C. M. Niu and N. Lan are with the Laboratory of Neuro-Rehabilitation Engineering, the School of Biomedical Engineering, Shanghai

Jiao Tong University, Shanghai, 200030, China (Luo e-mail: luoqi_ctp@sjtu.edu.cn; Niu e-mail: minos.niu@gmail.com; Lan e-mail: ninglan@sjtu.edu.cn).

C. M. Niu, N. Lan are also with the Institute of Medical Robotics, Shanghai Jiao Tong University, Shanghai, China.

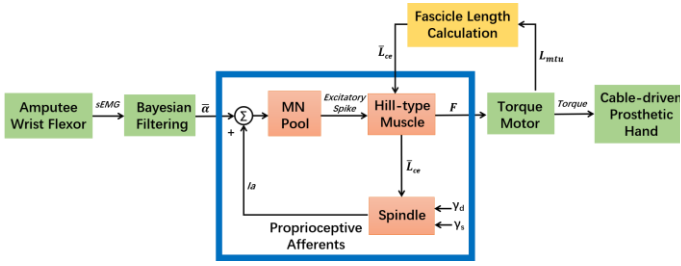


Figure 1. Block diagram of the model-based biomimetic controller. Wrist flexor EMG is filtered using a Bayesian algorithm, which eventually establishes the model-produced force on the torque motor; proprioceptive information is deduced from the torque motor to populate the muscle spindle.

and proximal interphalangeal (PIP) joints. The cables were attached to the shaft of a torque motor, which generated a torque resulting in a tension on the cable. Only finger flexion was activated by motor commands; finger extension was passively applied by an extending spring in each joint.

B. Model-based Biomimetic Controller for Prosthetic Hand

The architecture of model-based biomimetic controller is shown in Fig.1. Wrist flexor EMG from the amputee was filtered into the alpha motor command (α) by adopting a nonlinear Bayesian algorithm that had proven its advantage in myoelectric control applications [10]. The alpha motor command activated the biomimetic controller to compute for the expected tension. A torque motor established the expected tension with closed-loop adjustment from the neuromuscular reflex simulated in neuromorphic hardware. The torque motor pulled a tendon that flexed the prosthetic hand.

The biomimetic controller included models of motoneuron pool, skeletal muscle, and muscle spindle. We implemented a Hill-type model for muscle [11]. Spiking motoneurons were implemented following the Izhikevich model [12], which took the excitatory post-synaptic current as the input and produced a spike train as the output. Biomimetic proprioception was provided by implementing a physiologically realistic model of muscle spindle [4] with inputs of fascicle length, gamma (γ_d) dynamic and static (γ_s), and output of primary (I_a) afferents. Proprioceptive feedback on fascicle length was calculated from the shaft rotation of torque motor. Therefore, the monosynaptic spinal loop formed a closed-loop for regulating muscle tone and reflex. The detailed implementation of the biomimetic controller had been described in previous work [1].

C. Range of Fascicle Length for Biomimetic Controller

As shown in Fig.2, the muscle length (L_m) refers to the sum of the length of contractile element (L_{ce}) and the length of series elastic element (L_{se}). And the fascicle length (L_{ce}) is the length of the contractile element. L_m and L_{ce} are the key inputs to the muscle model and spindle mode respectively, as given by:

$$L_m(t) = L_m(0) - \Delta L_m \quad (1)$$

$$L_{ce}(t) = L_{ce}(0) - \Delta L_{ce} \quad (2)$$

where $L_m(t)$ and $L_{ce}(t)$ are the instantaneous length of muscle length and fascicle length. $L_m(0)$ and $L_{ce}(0)$ are the initial length, and ΔL_m and ΔL_{ce} are the changes in length.

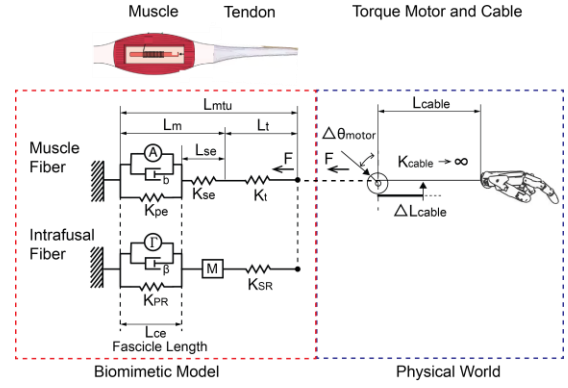


Figure 2. Muscle length information in the biomimetic muscle model and the interaction with the physical world.

1) Estimate ΔL_m from ΔL_{mtu}

In the biomimetic controller, the prosthetic hand flexion is realized by simulating the movement characteristics of flexor carpi ulnar (FCU). The stiffness of cable (K_{cable}) is assumed to be infinite, and its effect can be ignored, so that the change in the cable length (ΔL_{cable}) is equivalent to the change in the length of musculotendinous unit (ΔL_{mtu}) in the muscle model. The translational displacement of the cable can be measured by a rotational transducer on the torque motor (Fig.2).

$$\begin{aligned} L_{cable}(t) &= L_{cable}(0) - \Delta L_{cable} \\ &= L_{cable}(0) - r\Delta\theta_{motor} \end{aligned} \quad (3)$$

meaning that the instantaneous $L_{cable}(t)$ equals the length of the initial cable minus the cable length coiled on the winder ($\Delta\theta_{motor}$). $L_{cable}(0) = 39.7$ cm denotes the initial length of the cable, as determined by the placement of the motor on anatomical socket; $L_{cable}(0)$ is also similar to the length of a typical FCU MTU (38.3 cm) [13]. $r = 0.25$ cm denotes the radius of the cable winder.

As shown in Fig.2, the total stiffness of K_{se} and K_t in series is denoted as K . K_{se} is the stiffness of the series elastic element, K_t is the stiffness of tendon. When K_t approaches infinity, K is equal to K_{se} . Therefore, when K_t is large enough, the effect of K_t can be ignored, and K_{se} is approximately equivalent to K . In the biomimetic model, $K_{se} = 1.33$ N/cm [11], and $K_t = 1400$ N/cm [14]. K is almost equal to K_{se} , so ignoring the effect of K_t , it is a feasible approximation to equate ΔL_{mtu} to ΔL_m .

2) Estimate ΔL_{ce} from ΔL_{mtu}

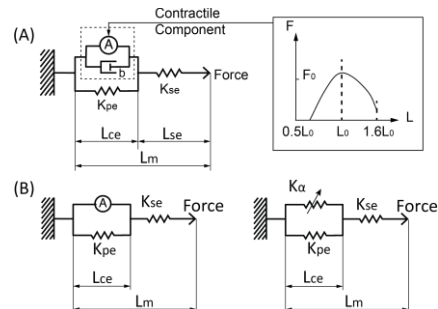


Figure 3. (A) Active force-length property in Hill-type muscle model. (B) By ignoring the damping in the contractile component, the muscle model reduces to the left scenario. We resolve L_{ce} by approximating the active component as a stiffness-adjustable spring (K_α , right).

When the finger is in contact with an object, we ignore the effect of muscle damping due to relative slow lengthening of the muscle (Fig.3B). Besides, the mass element of the intrafusal fiber was ignored when calculating L_{ce} . According to the force-length property [8], the active component in Hill-type muscle model is the equivalent of a spring with adjustable stiffness K_a . Therefore, according to the series-parallel characteristics of spring, ΔL_{ce} is given by:

$$\Delta L_{ce} = \frac{K_{se}}{K_{se} + K_{pe} + K_a} * \Delta L_{mtu} \quad (4)$$

The adjustable stiffness K_a can be inferred from the force-length relationship as follows:

$$K_a = \begin{cases} (-57.76\alpha + 60.24) * L_m + 57.41\alpha - 12.28, & L_m \leq L_m^o \\ (-14.61\alpha + 15.23) * L_m + 14.47\alpha - 32.31, & L_m > L_m^o \end{cases} \quad (5)$$

Therefore, the fascicle length can be calculated from eqs.2, 4 and 5. The calculated L_{ce} was normalized and sent to the muscle model and spindle model. **The normalized L_{ce} is obtained by dividing the calculated actual fascicle length (L_{ce}) by optimal length (L_o).**

3) Initial values of L_m and L_{ce}

R_1 (0.5 – 1.0 L_o): The initial value of L_m is 23.6 cm, and the initial value of L_{ce} is 1.0 L_o ($L_o = 2.2$ cm).

R_2 (0.5 – 1.3 L_o): The initial value of L_m is 23.6 cm, and the initial value of L_{ce} is 1.3 L_o ($L_o = 1.4$ cm).

R_3 (0.5 – 1.6 L_o): The initial value of L_m is 23.6 cm, and the initial value of L_{ce} is 1.6 L_o ($L_o = 1.0$ cm).

R_1 only works in the positive stiffness zone of the active component of muscle. R_2 was wider than R_1 , including both positive and negative muscle stiffness regions. R_3 was widest among all ranges, also containing the positive and negative muscle stiffness regions.

The active force-length property of muscle model in the biomimetic controller is shown in Fig.3A. The region where active muscle force A is generated is (nominally) $0.5 L_o < L_{ce} < 1.6 L_o$, where L_o is the length at which active muscle force peak. According to the active force-length property of muscle, the optimal length for force production (L_o) can reach the peak of muscle active force [8]. L_o is often used as a species-specific scaling factor (standard value of normalized muscle length) for calculation of the active component in the force-length (FL) curve [15].

D. Force Generation Test

Capability of force generation was tested using a finger-pressing task. The index finger of the prosthetic hand was activated to press down a force transducer (Model FNA, 0 – 30 N, Forsentek Co., Ltd., Shenzhen, China), which recorded the downward pressure (fingertip force) at 100 Hz with 12bit resolution (Model USB-201, Measurement Computing Corp., MA, U.S.).

As shown in Fig.4, the prosthetic finger was initially hovering at 1 cm above the force transducer ($D = 1$ cm). The prosthetic hand was fully extended at the beginning. Thereafter, a step alpha command ($U(t) = \text{Alpha} * 1(t)$) was issued to the biomimetic controller, which drove the prosthetic finger to move till the fingertip contact the force transducer.

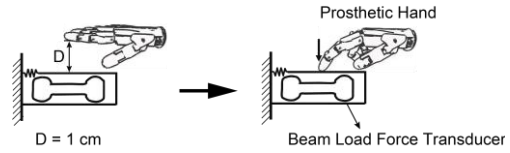


Figure 4. Experimental setup of generation capability test for the prosthetic hand.

III. RESULTS

A. Force Generation Capability of Prosthetic Finger

Fig.5 (A-C) shows the linear relationship between the force generated by the prosthetic finger and alpha motor command in different ranges of fascicle length, averaged across 3 measurements. With R_1 , the alpha motor command reached the maximum value of 1 when the generated force reached approximately 11.43 ± 0.09 N (Fig.5A). The linear relationship between the fingertip force and alpha command was significant ($R^2 = 0.989$, $p < 0.001$). Similarly, with R_2 , the alpha motor command reached the maximum value of 1 when the generated force was about 13.43 ± 0.09 N (Fig.5B). The linear relationship between the fingertip force and alpha command also was significant ($R^2 = 0.991$, $p < 0.001$). Also, when L_{ce} range was R_3 , the alpha motor command reached the maximum value of 1 and the force generated with the finger was approximately 14.97 ± 0.05 N (Fig.5C). The linear relationship between the fingertip force and alpha command was significant ($R^2 = 0.991$, $p < 0.001$).

Fig. 5 (D-F) shows the dynamic changes of L_{ce} when the alpha motor command reached the maximum value of 1 under three L_{ce} ranges. With R_1 , L_{ce} changed from the initial value 1.0 L_o to about 0.75 L_o . And with R_2 , L_{ce} changed from the initial value 1.3 L_o to approximately 0.87 L_o . With R_3 , L_{ce} changed from the initial value 1.6 L_o to about 1.02 L_o .

B. Dynamic Response of Prosthetic Hand

As shown in Fig.6, a step alpha command ($\text{Alpha} = 0.4$) was issued to the biomimetic controller (five repeated measurements), the force generated by the prosthetic finger in the three ranges was 4.14 ± 0.15 N, 5.24 ± 0.11 N, 5.84 ± 0.11 N. And the rise time was 0.756 ± 0.093 s, 0.690 ± 0.094 s, and 0.766 ± 0.092 s, respectively. There is no statistically significant difference in rise time between R_1 , R_2 , and R_3 ($p = 0.402$).

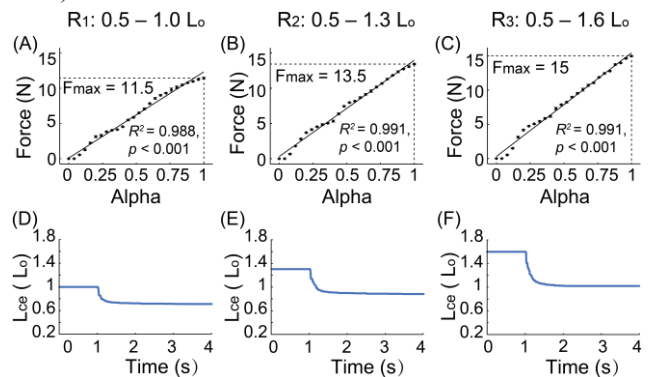


Figure 5. Under different fascicle length ranges (R_1 : 0.5 – 1.0 L_o ; R_2 : 0.5 – 1.3 L_o ; R_3 : 0.5 – 1.6 L_o), the prosthetic finger generation force in response to alpha motor command (A, B, C) and the dynamic change of L_{ce} when $\text{Alpha} = 1$ (D, E, F).

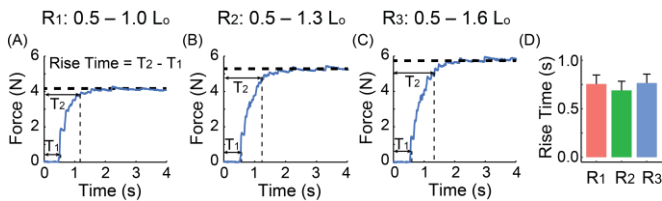


Figure 6. Dynamic responses of prosthetic hand received a step alpha command ($\alpha = 0.4$) in different fascicle length ranges. Rise time is the time required for the force response to rise from 10% to 90% of the steady-state force. There is no statistically significant difference in rise time between R_1 , R_2 , and R_3 ($p = 0.402$).

The rise time of the prosthetic finger to produce a same target force under three L_{ce} ranges is shown in Fig.7. The prosthetic finger generated a target force of 8 N (five repeated measurements), and the alpha commands to be sent to the system are 0.65, 0.6, and 0.55, respectively. The rise time in the three ranges was 0.488 ± 0.019 s, 0.484 ± 0.025 s, and 0.508 ± 0.038 s. There is no statistically significant difference in rise time between R_1 , R_2 , and R_3 ($p = 0.402$).

IV. DISCUSSION

We explored the effect of fascicle length range on force generation capability of the biomimetic controller for a tendon-driven prosthetic hand. The steady state force output and transient force responses were evaluated with a range of step inputs as controller input. Three ranges of fascicle length were compared, and results showed that the prosthetic finger could produce a linear steady force output response with all 3 ranges of fascicle length. Peak force of the prosthetic hand was the largest with R_3 , followed by R_2 and R_1 . Fascicle length range had no significant effect on the rise time in force generation tasks. Our results supported that centering fascicle length around the optimal length (L_o) may result in greater force generation during reflex-enabled prosthetic control.

The muscle active force is deemed to depend on the current fascicle length and velocity, the state of activation of muscle fibers [7], [8]. The muscle force was solely determined by fascicle length, since in our test of force generation the alpha motor commands (state of activation) were constant and the velocity was zero. It can be seen from Fig.5 (D-F) that when the alpha motor command is at its maximum, the closer the fascicle length to $1.0 L_o$ resulted in greater force generation.

Nevertheless, in the force generation task, the prosthetic finger touched the force transducer, and the fascicle length well fell near the optimal length (L_o) region so that the maximum force was generated. This force generation way of the prosthetic hand has obvious limitations. Because in the actual grip tasks, the contact point of force control could not ensure that the fascicle length could vary around the optimal length, so the fascicle length range may have different effects on the prosthetic hand grasping objects with various sizes and shapes.

V. CONCLUSION

This study shows that when the fascicle length centers around the optimal length (L_o) during reflex-enabled prosthetic control, the hand may produce greater force during

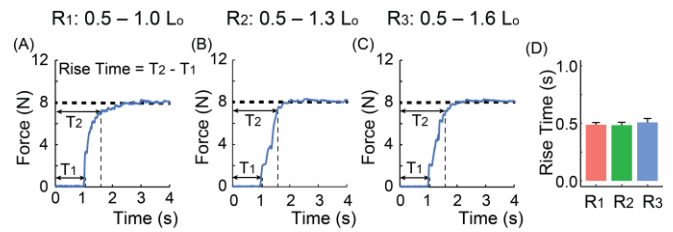


Figure 7. Dynamic responses of prosthetic hand generating the same target forces (8 N) in different fascicle length ranges. The prosthetic hand generated a target force of 8 N, and the alpha commands to be sent to the system are different in the three ranges; (A) $\alpha = 0.65$; (B) $\alpha = 0.6$; (C) $\alpha = 0.55$. (D) Rise time is the time required for the force response to rise from 10% to 90% of the steady-state force. Rise time is no statistically significant difference in R_1 , R_2 , and R_3 ($p = 0.402$).

grasping tasks. However, the finding may not generalize to arbitrary tasks, since the instantaneous fascicle length depends also on the interaction between environment and amputee.

REFERENCES

- [1] C. M. Niu, Q. Luo, C. Chou, J. Liu, M. Hao, and N. Lan, "Neuromorphic Model of Reflex for Realtime Human-Like Compliant Control of Prosthetic Hand," *Annals of Biomedical Engineering*, Aug. 2020.
- [2] Q. Luo *et al.*, "Design of a Biomimetic Control System for Tendon-driven Prosthetic Hand," in *2018 IEEE International Conference on Cyborg and Bionic Systems (CBS)*, Shenzhen, Oct. 2018, pp. 528–531.
- [3] J. C. Houk, W. Z. Rymer, and P. E. Crago, "Dependence of dynamic response of spindle receptors on muscle length and velocity.," *Journal of Neurophysiology*, vol. 46, no. 1, pp. 143–166, Jul. 1981.
- [4] M. P. Mileusnic, I. E. Brown, N. Lan, and G. E. Loeb, "Mathematical Models of Proprioceptors. I. Control and Transduction in the Muscle Spindle," *Journal of Neurophysiology*, vol. 96, no. 4, pp. 1772–1788, Oct. 2006.
- [5] D. Song, N. Lan, G. E. Loeb, and J. Gordon, "Model-Based Sensorimotor Integration for Multi-Joint Control: Development of a Virtual Arm Model," *Annals of Biomedical Engineering*, vol. 36, no. 6, pp. 1033–1048, Jun. 2008.
- [6] N. Lan and X. He, "Fusimotor control of spindle sensitivity regulates central and peripheral coding of joint angles," *Frontiers in Computational Neuroscience*, vol. 6, 2012.
- [7] A. V. Hill, "The heat of shortening and the dynamic constants of muscle," *Proceedings of the Royal Society of London. Series B-Biological Sciences*, p. 60, 1938.
- [8] F. E. Zajac, "Muscle and tendon: properties, models, scaling, and application to biomechanics and motor control," *Crit Rev Biomed Eng*, vol. 17, no. 4, pp. 359–411, 1989.
- [9] E. J. Cheng, I. E. Brown, and G. E. Loeb, "Virtual muscle: a computational approach to understanding the effects of muscle properties on motor control," *Journal of Neuroscience Methods*, vol. 101, no. 2, pp. 117–130, Sep. 2000.
- [10] T. D. Sanger, "Bayesian Filtering of Myoelectric Signals," *Journal of Neurophysiology*, vol. 97, no. 2, pp. 1839–1845, Feb. 2007, doi: 10.1152/jn.00936.2006.
- [11] R. Shadmehr and S. P. Wise, *A Mathematical Muscle Model..In Supplementary documents for "Computational Neurobiology of Reaching and Pointing."* MIT Press, 2005.
- [12] E. M. Izhikevich, "Simple model of spiking neurons," *IEEE transactions on neural networks*, vol. 14, no. 6, pp. 1569–1572, 2003.
- [13] J. Fridén, R. M. Lovering, and R. L. Lieber, "Fiber length variability within the flexor carpi ulnaris and flexor carpi radialis muscles: implications for surgical tendon transfer," *The Journal of Hand Surgery*, vol. 29, no. 5, pp. 909–914, Sep. 2004.
- [14] C. S. Cook and M. J. N. McDonagh, "Measurement of muscle and tendon stiffness in man," *Europ. J. Appl. Physiol.*, vol. 72, no. 4, pp. 380–382, 1996.
- [15] I. E. Brown and T. L. Liinamaa, "Relationships between range of motion, L_o , and passive force in five strap-like muscles of the feline hind limb," *Journal of morphology*, p. 9, 1996.